

Rezūm System Water Vapor Treatment for Lower Urinary Tract Symptoms/Benign Prostatic Hyperplasia: Validation of Convective Thermal Energy Transfer and Characterization With Magnetic Resonance Imaging and 3-Dimensional Renderings



Lance A. Mynderse, Dennis Hanson, Richard A. Robb, Dalibor Pacik, Viteslav Vit, Gabriel Varga, Lennart Wagrell, Magnus Tornblom, Edwin Rijo Cedano, David A. Woodrum, Christopher M. Dixon, and Thayne R. Larson

OBJECTIVE	To evaluate by magnetic resonance imaging the physical effects of convective thermal energy transfer with water vapor as a means of treating lower urinary tract symptoms due to benign prostatic hyperplasia.
METHODS	Sixty-five men with lower urinary tract symptoms were treated with the Rezūm System by transurethral intraprostatic injection of water vapor. A group of 45 of these men consented to undergo a series of gadolinium-enhanced magnetic resonance imagings of the prostate after treatment to monitor the size and location of ablative lesions, their time course of resolution, and the corresponding change in prostate tissue volume. Visualization was conducted at 1 week, 1, 3, and 6 months after treatment.
RESULTS	Outcomes were available for 44 patients. Convective thermal lesions were limited to the transition zone and correlated with targeted treatment locations. At 1 week after treatment, the mean volume of ablative lesions was 8.2 cm ³ (0.5-24.0 cm ³). At 6 months, whole prostate volume was reduced by a mean of 28.9% and transition zone volume by 38.0% as compared with baseline 1-week images. At 3 and 6 months after treatment, the lesion volumes had reduced by 91.5% and 95.1%, respectively. Lesions remained within the targeted treatment zone without compromising integrity of the bladder, rectum, or striated urinary sphincter.
CONCLUSION	This imaging study confirms the delivery of convective water vapor technology to create thermal lesions in the prostate tissue. Lesions generated underwent near complete resolution by 3 and 6 months after treatment with a concomitant one-third reduction in overall prostate and transition zone volumes. UROLOGY 86: 122–127, 2015. © 2015 Elsevier Inc.

Benign prostatic hyperplasia (BPH) is one of the most common and costly disorders of older men associated with a wide range of lower urinary tract symptoms (LUTS) that can significantly affect a

man's quality of life.¹ By 70 years of age, nearly 70% of men will have the histologic findings of periurethral, glandular, and cellular element proliferation of the prostate, with about half of these men developing

Financial Disclosure: Dalibor Pacik, Viteslav Vit, Gabriel Varga, Lennart Wagrell, Magnus Tornblom, and Edwin Rijo Cedano are clinical trial investigators for NxThera, Inc. Christopher M. Dixon and Thayne R. Larson are consultants for NxThera, Inc. Richard Robb, Dennis Hanson and Mayo Clinic have a financial interest in the Analyze II.0 image analysis technology used in this research.

Funding Support: This study was funded by NxThera, Inc.

From the Department of Urology, Mayo Clinic, Rochester, MN; the Biomedical Imaging Resource, Mayo Clinic, Rochester, MN; the Department of Urology, University

Hospital Brno, Brno, Czech Republic; the Urologcentrum, Stockholm, Sweden; the Department of Urology, Clinica Canela, La Romana, Dominican Republic; the Department of Radiology, Mayo Clinic, Rochester, MN; the Department of Urology, Lenox Hill Hospital, New York, NY; and the Institute of Medical Research, Scottsdale, AZ

Address correspondence to: Lance A. Mynderse, M.D., Department of Urology, Mayo Clinic, 200 1st St SW, Rochester, MN 55905. E-mail: mynderse.lance@mayo.edu

Submitted: February 5, 2015, accepted (with revisions): March 23, 2015

prostatic enlargement leading to bladder outlet obstruction.² The prevalence of histologic BPH is similar in Asia, Europe, and the United States.³ In the past 3 decades, this common ailment has led many men to seek minimally invasive technologies to treat LUTS secondary to BPH. A number of such therapeutic options have been introduced, including radiofrequency (RF), microwave, and laser therapies.

The Rezūm System (NxThera, Inc., Maple Grove, MN) is a unique, minimally invasive, transurethral therapy using Convective Water Vapor Energy (WAVE), which uses RF to create thermal energy in the form of water vapor. This therapy involves transurethral thermal energy transfer using the convective properties of water vapor, releasing large amounts of stored thermal energy (540 cal/mL H₂O) as the water vapor contacts tissue and condenses back into water. The water vapor disperses swiftly and uniformly through the tissue interstices when injected at slightly above interstitial pressure, disrupting cell membranes without a discernible thermal gradient.⁴ Traditional minimally invasive therapies for BPH-LUTS have relied on conduction of large amounts of thermal energy from a central source at higher temperature to a lower one, heating tissue within the treatment zone.⁴ Thermodynamically, conductive heat transfer requires long treatment times and considerable energy deposition to effect tissue destruction with an obligatory temperature gradient.⁵

Lesion characterization is necessary in considering the potential of a new ablative technology. Previous publications have correlated gadolinium defects on magnetic resonance imaging (MRI) with regions of reduced or absent blood flow.⁶ These defects correspond to cell death, as seen with whole mount histopathology, and are consistent with thermal ablative effects.^{6,7} Such approaches have been used to characterize a number of thermal therapies for the treatment of BPH-LUTS.⁸⁻¹² Lesion visualization helps the clinician understand the effects of treatment on the surrounding tissues, dosage adequacy, and lesion location in relation to the placement of the needle and the ablative region.

The objective of the study was to evaluate the physical effects of convective thermal energy transfer of water vapor to treat prostatic tissue in patients with BPH-LUTS and to assess the MRI-detected thermal lesion characteristics and their resolution with serial MRI.

METHODS

Local ethics committee approval was received for a series of pilot studies conducted at 3 sites (Dominican Republic, Czech Republic, and Sweden) involving 65 consented patients all of whom underwent the convective water vapor energy treatment of LUTS due to BPH. The first 20 patients were treated in the Dominican Republic, the next 18 in the Czech Republic, and the final 27 in Sweden. The water vapor energy treatment system included a generator and a single-use transurethral water vapor delivery device that incorporated a standard rigid

30° cystoscope lens, which allowed the procedure to be performed under direct visualization. Hand-held controls in the device were used to deliver vapor through an 18g needle and saline flush for visualization and to cool the urethra during treatments. With the patients in a lithotomy position, the water vapor delivery device was inserted into the urethra. The polyether ether ketone (PEEK) vapor needle was deployed under direct visualization into the transition zone of the prostate, and water vapor was delivered through 12 small emitter holes spaced around the PEEK needle at 120° intervals, allowing for the circumferential dispersion of water vapor into the tissue. The sterile water vapor was delivered in injections averaging 9 seconds (range, 7-10 seconds) duration into the tissue commencing approximately 1 cm from the bladder neck at the 3- and 9-o'clock positions. Additional injections of vapor were delivered every 0.5-1.0 cm from the initial injection site caudally down the length of the prostatic urethra to the proximal edge of the verumontanum. When present, the median lobe was treated with 1-3 injections. The total number of water vapor injections in each lobe of the prostate was determined by the size of the adenoma and length of the prostatic urethra.

As per the original pilot study design, 45 of these patients were subjected to 4, modified, multiparametric gadolinium-enhanced MRI sequences of the prostate and pelvis at 1 week, 1, 3, and 6 months after convective water vapor energy treatment. The 1-week MRI was used to assess the acute treatment effect including size, location, and extent of the ablation due to the water vapor injections. The remaining follow-up imaging sequences allowed the evaluation of lesion resolution with time. Overall prostate and transition zone volumes were measured over the time course. All images were used to document safety of the surrounding tissues.

Patient MRI scans were conducted on 3 different make 1.5-T scanners at the 3 clinical study sites (Dominican and Czech Republics: Toshiba Vantage Titan; Sweden: Philips Intera, and Siemens MAGNETOM Aera). Acquisition protocols were standardized across each site within the limits of the different scanner manufacturers. Precontrast sequences included axial T1 and axial, coronal, and sagittal T2. Dynamic contrast-enhanced T1 axial acquisitions were initiated 10 seconds after contrast administration, with multiple (2-10) repeated fast acquisitions (range, 23-134 seconds) performed to capture maximal contrast enhancement. Postcontrast axial, coronal, and sagittal T1 acquisitions were performed after the dynamic sequence. The precontrast axial T2 and dynamic axial T1 showing maximal contrast uptake were used in the volumetric analysis. Postcontrast coronal and sagittal T1 acquisitions were used to evaluate lesion location relative to the bladder neck and rectal wall. Image analysis was conducted using Analyze 11.0 (Biomedical Imaging Resource, Mayo Clinic, Rochester, MN), a visualization and analysis application capable of image segmentation, processing, registration and multimodality fusion, mensuration, and volume rendering.

MRI data were analyzed by a central lab under the guidance of an independent urologist and radiologist at the Biomedical Imaging Resource, Mayo Clinic in Rochester, MN. The segmented MRI volumes were processed into 3D volume renderings depicting whole prostate, transition zone, and treatment lesions. These renderings allowed further visualization of lesion location in relation to prostate zonal anatomy and lesion resolution over time.

Table 1. Outcome after convective water vapor therapy including magnetic resonance imaging—detected measures of whole prostate volumes, transition zone, and lesion size, at 1 week, 1, 3, and 6 months after treatment

Variable	Time	N	Mean (Range)	Mean (Range) Δ	Mean % Δ
Whole prostate volume (cm ³)	1 wk	44	61.2 (20.4-133.2)		
	1 mo	42	52.7 (15.4-118.4)	−8.5	−13.9
	3 mo	41	47.0 (15.3-115.4)	−14.2	−23.2
	6 mo	40	43.5 (16.0-116.6)	−17.7	−28.9
Transition zone volume (cm ³)	1 wk	44	36.3 (9.1-87.8)		
	1 mo	42	29.8 (8.4-80.3)	−6.5	−17.9
	3 mo	41	25.1 (6.8-79.4)	−11.2	−30.9
	6 mo	40	22.5 (6.6-79.3)	−13.8	−38.0
Gadolinium defect lesion volume (cm ³)	1 wk	44	8.2 (0.5-24.0)		
	1 mo	42	3.4 (0.3-11.3)	−4.8	−58.5
	3 mo	41	0.7 (0.0-2.6)	−7.5	−91.5
	6 mo	40	0.4 (0.0-3.7)	−7.8	−95.1

RESULTS

For the evaluable treatment cohort of 44 patients, the post-treatment volume of gadolinium defects, as well as the prostate and transition zone volumes, is shown in Table 1. Susceptibility artifact distortion from 1 patient's prosthetic hip implant prevented image analysis of 1 of the 45 patients. The mean number of injections into each lateral lobe was 2.0 (range, 1-4). At 6 months, whole prostate volume was reduced by a mean of 28.9% (−17.7 cm³) and transition zone volume by 38.0% (−13.8 cm³) as compared with that of baseline 1-week images. The size of the gadolinium defect reduced with time such that at 6 months, the mean size of the lesion was reduced by 95.1% (−7.8 cm³).

Twelve of the 44 patients with a baseline mean (range) prostate size of 31.5 cm³ (20.8-43.4 cm³), as measured by transurethral ultrasound, received only 1 injection per lateral lobe due to the prostate size and prostatic urethral length. The average lesion volume in this subset was 1.7 cm³ (0.2-4.1 cm³) per lobe. This lesion volume compares with a mean of 4.8 cm³ (0.8-16.8 cm³) per lobe when >1 water vapor injection per lobe was delivered.

In those prostatic lobes treated with >1 water vapor injection, the gadolinium defects coalesced, evidencing contiguous ablative lesions with a documented resorption of ablative lesions over time (Fig. 1). The lesions remained within the area between the bladder neck and the verumontanum within the transition zone (Fig. 2A). Also, most prostatic urethra could be visualized by the gadolinium-enhanced areas on coronal views and appear preserved (Fig. 2B). An average of 1.3 (range, 1-2) water vapor injections was given to 6 patients with treated median lobes, and the average volume of gadolinium defect was 1.5 cm³ (0.4-3.0 cm³). In each case, lesions are seen within the median lobe (Fig. 2C).

In 3 patients, MRI images at 1 week showed that some treatment energy was delivered outside the prostate target. The subsequent 1-, 3-, and 6-month images showed progressive and complete resolution of the extraprostatic treatment. No negative sequelae were witnessed in this small group of patients.

The closest distance of each lesion to the rectal wall was measured. In no case was a lesion seen between the prostate and the rectal wall. The mean closest distance of lesions to the rectal wall for all patients was 15.4 mm (range, 5.2-62.2 mm). The treatment defects were within 1-4 mm of the urethra and the prostatic urethral mucosa, appeared intact, as demonstrated by the gadolinium-enhanced areas on coronal views (Fig. 1).

Three of the 44 patients had before treatment, baseline MRIs to assess overall prostate and transition zone edema. The percentage overall volume change from the baseline in these patients was 15%.

Matched-pair prostate-specific antigen (PSA) levels at the baseline and during follow-up are shown in Table 2. One-week after treatment, PSA levels increased 5-fold but at 3 months, values were similar to those at the baseline.

COMMENT

Gadolinium-enhanced MRIs of the prostate have been used to characterize the ablative lesions of BPH-LUTS thermal technologies and their resolution over time. However, all previous MRI characterizations of prostate tissue ablations have been exclusively created by conductive thermal heat transfer and injury. We have previously reported MRIs of the ablative zones created by convective thermal energy transfer using water vapor energy,¹³ but this study images the lesions and observes the resorption of these lesions during follow-up. When multiple water vapor injections were used, the ablative lesions appeared to coalesce within the transition zone. The 1-week post-treatment MRIs clearly show large ablative lesions created within the lateral and median lobes using water vapor injections delivering an average 416 calories (range, 208-832 calories) per lobe. Thermal water vapor rapidly disperses through tissue interstices and deposits high caloric energy onto the cell membranes.¹⁴ Almost instantly, the membranes are denatured, rendering the cell unviable followed by necroptosis. If thermal water vapor treatment continues, the cells become heated throughout resulting in tissue coagulation and necrosis. Because of water vapor's convective mass transfer of wet thermal energy, as opposed to desiccating

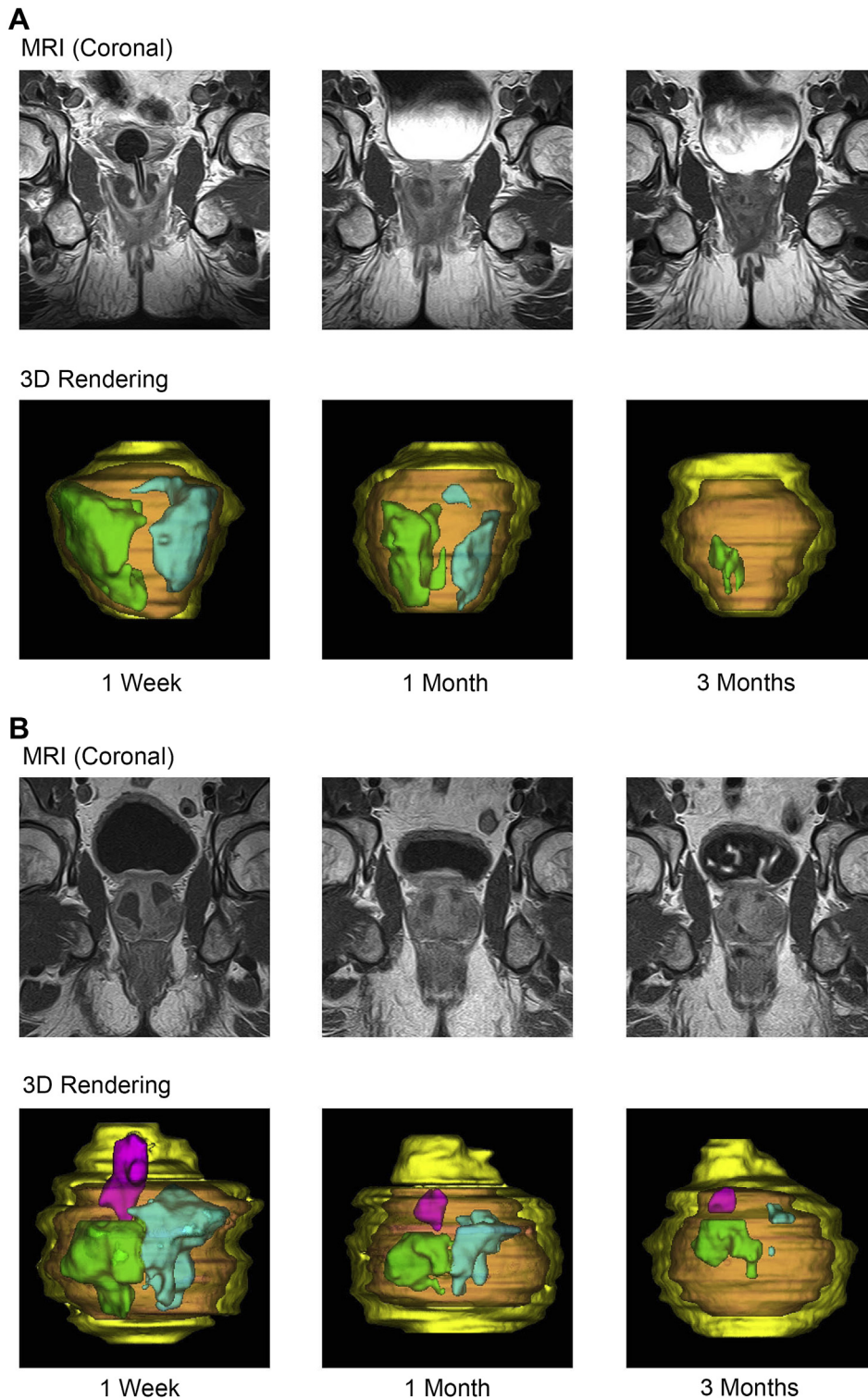


Figure 1. Magnetic resonance imaging of lesions generated by convective water vapor energy and their resolution after treatment. Three-dimensional renderings correspond to magnetic resonance imaging coronal views. Represented are the transition zone (orange) and lesions within the right lateral lobe (green), the left lateral lobe (blue), and the median lobe (pink). **(A)** Outcome at 1 week, 1 month, and 3 months after procedure demonstrating coalesced, contiguous lesion defect in a 39-cm³ prostate. **(B)** Outcome demonstrating more significant lesion defects in an 89-cm³ prostate. In both cases, by 3 months, most of the lesion volume had been resorbed. MRI, magnetic resonance imaging; 3D, 3-dimensional.

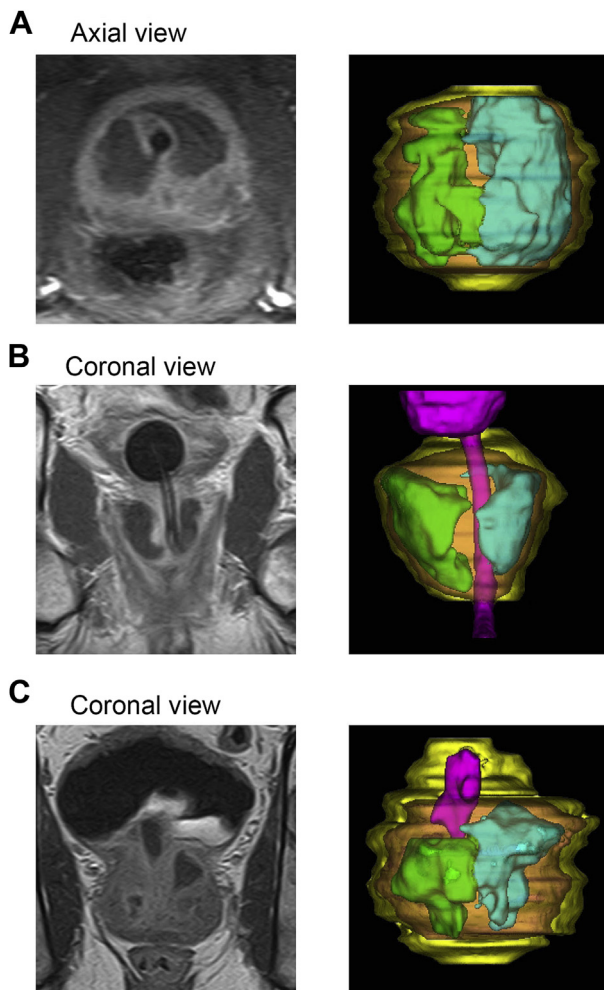


Figure 2. Magnetic resonance imaging of lesions generated by convective water vapor energy and their resolution at 1 week after treatment. Three-dimensional renderings correspond to magnetic resonance imaging coronal views. Represented are the transition zone (orange) and lesions within the right lateral lobe (green), the left lateral lobe (blue), and the median lobe (pink). **(A)** Boundaries of transition and peripheral zones and coalescing lesions stretching from the bladder neck to the verumontanum, **(B)** preservation of the prostatic urethra with lesions stretching from the bladder neck to the verumontanum, **(C)** treatment of lateral and median lobes.

electromagnetic energy such as RF and microwave, there is little tissue shrinkage or fixation, and resorption is almost complete.¹⁴ The thermal fixation often associated with RF or microwave generally lacks a wound healing response, resists breakdown or tissue repair, and may elicit a localized foreign body—type reaction.^{15,16}

A unique aspect seen in the imaging of convective water vapor treatment of the prostate is the manner in which the energy deposition is contained within the zonal boundaries of glandular anatomy. Delivering 208 calories per water vapor injection, with proper positioning of the PEEK needle into the transition zone, the water vapor dispersed within the transition zone, but it

did not penetrate the densified tissue boundary separating the peripheral and transition zones and was contained within the transition zone. This property of convective heat transfer in water vapor therapy is very different than conductive thermal therapies that do not recognize tissue boundaries.

Another feature of this technology is the short treatment duration. The 1-week post-treatment MRIs clearly show large ablative lesions created within the transition zone using total vapor injection treatment times from 18 to 72 seconds. Lesions using conductive thermal technologies such as microwave, RF, or interstitial laser require a minimum of 10 times the thermal exposure time to achieve a comparable effect. The magnetic resonance images also highlight the safety characteristics of water vapor. The water vapor treatments appear safe on imaging, with lesions remaining within the zone targeted without compromising the integrity of the bladder, rectum, or striated urinary sphincter.

Convective water vapor energy allows physician-directed positioning of the energy and the number of treatments to be delivered, including treatment of median and asymmetric lateral lobes. This study represents the first evaluation of the MRI characteristics of convective thermal therapy in the prostate. By imaging soon after treatment at 1 week and at subsequent evaluation intervals, a detailed time course of the prostate anatomy was documented. Using the Analyze software for 3-dimensional renderings of the whole prostate, transition zone, and ablative lesions, the precise relationship of the treatment lesion to the bladder neck, apex, and peripheral zone can be visualized. Furthermore, as each treatment cystoscopy was video recorded, PEEK needle placement and subsequent MRI volume analysis could be reconciled.

A distinctive feature of convective heat transfer in the prostate appears to be the time course of the ablative lesion resolution. This detailed imaging analysis of convective lesion resolution after treatment of BPH-LUTS shows significant resolution by 3 months (91.5%) and nearly complete resolution (95.1%) of the ablative lesion by 6 months. Using data from the 12 patients with smaller prostates who received a single injection of water vapor per lateral lobe, we gain insight into the necrotic volume caused by this single water vapor injection. Each 208-calorie injection of vapor energy equated to a mean lesion size of 1.7 cm³ per lateral lobe. The predictability of lesion size is surely dependent on multiple factors, including, but not limited to, the shape of tissue boundaries, interstitial pressure, and density of the target tissue.

Although the total prostate volume was reduced by 28% at 6 months, the serum PSA level was unchanged at 3 and 6 months. The first PSA level at 1-week after therapy clearly shows significant treatment effect, but at later time points likely reflects the limited inflammatory effect caused by water vapor therapy and the minimally invasive nonresective character of this technology.

Table 2. Paired PSA levels at the baseline and during 6 months of follow-up

	Time Point			
	1 wk	1 mo	3 mo	6 mo
PSA (ng/mL)				
N (paired values)	36	20	41	41
Baseline	3.5 (3.6)	4.3 (4.1)	3.3 (3.4)	3.3 (3.4)
Follow-up	18.7 (16.0)	5.6 (3.3)	3.3 (3.8)	3.1 (3.0)
Change	15.2 (15.3)	1.2 (3.5)	-0.0 (2.5)	-0.2 (1.9)
% Change (95% CI)	698.6 (429.4 to 967.8)	72.1 (23.1 to 121.2)	5.8 (-9.6 to 21.2)	4.6 (-10.5 to 19.6)
P value	<.001	.131	.971	.513

CI, confidence interval; PSA, prostate-specific antigen.
Mean (standard deviation) values are shown.

Although the decrease in prostate and transition zone volumes were significant over the course of 6 months, the exact amount of immediate swelling after procedure is not known, therefore making the absolute amount of shrinkage of the prostate and transition zone difficult to quantify. Further limitations of this study include the potential error created by using similar but different MRI sequences unique to each of 3 different 1.5-T MRI scanners at the various treatment sites involved in this study. Substantial effort was made at the centralized image analysis site to integrate the image quality and minimize the effect of this variable. Strengths of this study include the multicenter nature of the treatments; the robust number of prostates treated, imaged, and analyzed; and the extensive MRI data set acquired over 6 months after treatment.

CONCLUSION

This multicenter study confirmed the principle of convective water vapor energy transfer to create thermal lesions in the prostatic tissue. Lesions generated underwent near complete resolution by 3 and 6 months after treatment with concomitant reduction in overall prostate and transition zone volumes as compared with the MRI measurements at 1 week. Lesions remained within the zone targeted without compromising integrity of the bladder, rectum, or striated urinary sphincter. Clinical outcome from the study is reported separately.

Acknowledgment. The authors acknowledge the contributions of Michael Hoey for his invention of and developments of both the underlying technology of and the therapy algorithms for the Rezüm System. We would like to acknowledge Jan Krístek, M.D., Ph.D., at SurGal Clinic for his contributions to the magnetic resonance imaging work and also, MedSciMedia, Ltd, for their editorial support.

References

1. Wei JT, Calhoun E, Jacobsen SJ. Urologic diseases in America project: benign prostatic hyperplasia. *J Urol.* 2008;179(suppl 5):S575-S580.

2. Berry SJ, Coffey DS, Walsh PC, Ewing LL. The development of human benign prostatic hyperplasia with age. *J Urol.* 1984;132:474-479.
3. Hollingsworth JM, Wilt TJ. Lower urinary tract symptoms in men. *BMJ.* 2014;349:g4474.
4. Hahn DW, Özişik MN. *Heat Conduction Fundamentals, in Heat Conduction.* 3rd ed. Hoboken, NJ, USA: John Wiley & Sons, Inc; 2012.
5. Bhowmick P, Coad JE, Bhowmick S, et al. In vitro assessment of the efficacy of thermal therapy in human benign prostatic hyperplasia. *Int J Hyperthermia.* 2004;20:421-439.
6. Osman YM, Larson TR, El-Diasty T, Ghoneim MA. Correlation between central zone perfusion defects on gadolinium-enhanced MRI and intraprostatic temperatures during transurethral microwave thermotherapy. *J Endourol.* 2000;14:761-766.
7. Larson BT, Collins JM, Huidobro C, et al. Gadolinium-enhanced MRI in the evaluation of minimally invasive treatments of the prostate: correlation with histopathologic findings. *Urology.* 2003;62:900-904.
8. Larson BT, Robertson DW, Huidobro C, et al. Interstitial temperature mapping during ProLieve transurethral microwave treatment: imaging reveals thermotherapy temperatures resulting in tissue necrosis and patent prostatic urethra. *Urology.* 2006;68:1206-1210.
9. Huidobro C, Bolmsjö M, Larson T, et al. Evaluation of microwave thermotherapy with histopathology, magnetic resonance imaging and temperature mapping. *J Urol.* 2004;71:672-678.
10. Larson T, Huidobro C, Acevedo C, et al. In vivo temperature mapping of prostate during treatment with TherMatrx TMx-2000 device: heat field and MRI determinations of necrotic lesions. *J Endourol.* 2005;19:1021-1025.
11. Mynderse LA, Larson B, Huidobro C, et al. Characterizing TUNA ablative treatments of the prostate for benign hyperplasia with gadolinium-enhanced magnetic resonance imaging. *J Endourol.* 2007;21:1361-1366.
12. Huidobro C, Larson B, Mynderse S, et al. Characterizing Prostiva RF treatments of the prostate for BPH with gadolinium-enhanced MRI. *ScientificWorldJournal.* 2009;9:10-16.
13. Dixon CM, Cedano ER, Mynderse LA, Larson TR. Transurethral convective water vapor as a treatment for lower urinary tract symptomatology due to benign prostatic hyperplasia using the Rezüm® system: evaluation of acute ablative capabilities in the human prostate. *Res Rep Urol.* 2015;7:13-18.
14. NxThera data on file.
15. Coad JE, Josari K, Humar A, Sielaff TD. Radiofrequency ablation causes 'thermal fixation' of hepatocellular carcinoma: a post-liver transplant histopathologic study. *Clin Transplant.* 2003;17:377-384.
16. Coad JE. Thermal fixation: a central outcome of hyperthermic therapies. *Prog Biomed Opt Imag.* 2005;5698:14-22.